Numerical simulation analysis of flow boiling heat transfer in internal micro-finned tubes

Yan Liu [1], Qiang Zhou [2], Huafeng Pan [2], Jingzhi Zhang [1] and Li Lei [1, *]

[1] School of Energy and Power Engineering, Shandong University, Jinan 250061, China

[2] Shanghai JHEAT Technology CO., LTD, Shanghai 201899, Shanghai China

*Corresponding author e-mail: leili@sdu.edu.cn

Abstract. Internal micro-finned tubes are widely used in modern air conditioning and refrigeration systems due to their excellent thermal performance during two-phase flow conditions. This study begins with a numerical simulation that examines the boiling heat transfer and two-phase flow characteristics of different refrigerants—R32, R410A, and R1234ze—inside a micro-finned tube with a 3.32 mm internal diameter. Subsequently, the paper presents a numerical analysis of R32's behavior in micro-fin tubes of identical diameter under heat flux densities of 10 kW/m2, 50 kW/m2, and 100 kW/m2, respectively. The results show that as various refrigerants flow and boil in the tubes, there is a sequential occurrence of bubble flow, slug flow, and wavy-annular flow. The boiling heat transfer coefficient is highest for R32 and lowest for R1234ze, with a direct proportionality to the refrigerant's latent heat of vaporization and liquid thermal conductivity. The local pressure drop escalates with increasing tube length, with R32 experiencing the highest average pressure drop, followed by R1234ze and R410A. Furthermore, the heat transfer coefficient diminishes as the heat flux density increases, while the pressure drop surges in response to rising heat flux density.

Keywords: internal microfinned tube, thermal performance, numerical simulation.

1. Introduction

Enhanced heat transfer technology has received widespread attention in air conditioning, heat dissipation, refrigeration systems, chemical processes, and some extreme heat transfer fields [1-4]. Internal micro-finned tubes are widely used in modern air conditioning and refrigeration systems due to their excellent thermal properties in two-phase flow. In recent years, there have been many studies on boiling heat transfer in tubes. Many scholars have studied the boiling heat transfer coefficient, pressure drop and flow pattern of refrigerant flow in tubes.

In terms of flow boiling heat transfer, Righetti et al. [5] conducted an experimental study on flow boiling of R1233zd(E) in a micro-fin tube with an inner diameter of 4.3 mm. They found that the heat transfer process of the flow boiling phenomenon is mainly affected by nucleation boiling and two-phase Forced convection is controlled by two mechanisms. Kondou et al. [6] experimentally studied the flow boiling of refrigerant R32/R1234ze(E) in a horizontal micro-fin tube with an inner diameter of 5.21mm. They found that the heat transfer coefficient of R32 alone was higher than that of R1234ze(E).

Many scholars have conducted extensive research on the pressure drop characteristics of microchannels. For example, Longo et al. [7] studied the boiling heat transfer characteristics of R32 and R410A in 4.2mm inner diameter micro-fin tubes, and found that the boiling heat transfer coefficient and friction pressure drop of R32 were 10-20% higher than that of R410A, which is a valuable low GWP alternative. Yang et al. [8] conducted experimental studies on the flow boiling heat transfer and pressure drop of refrigerants HFO1234yf and HFC-134a in small round tubes, and found that the pressure drop and flow boiling heat transfer performance are related to fluid properties, flow conditions and flow patterns.

In terms of two-phase flow patterns, Jige et al. [9] experimentally observed the flow pattern at the outlet of a micro-fin tube and divided it into two flow patterns: wavy slug flow and annular flow. Yu et al. [10] studied the flow patterns and heat transfer characteristics during the evaporation process of smooth tubes and micro-finned tubes with a diameter of 10.7 mm, and discussed the relationship

between flow patterns and local heat transfer coefficients. Kattan et al. [11] proposed a new boiling heat transfer model in horizontal plane tubes by analyzing the effects of local two-phase flow patterns, flow stratification and partial drying in annular flow.

Researchers both domestically and internationally have conducted extensive experimental research on the heat transfer characteristics of refrigerants in tubes. However, there is a lack of related numerical simulations focusing on different refrigerants in internal micro-finned tubes. This paper addresses this gap by performing a three-dimensional unsteady-state numerical simulation study on the boiling heat transfer of refrigerants R32, R410A, and R1234ze in an internal micro-finned tube with an inner diameter of 3.32mm. Subsequently, a three-dimensional unsteady numerical simulation study was carried out specifically on the boiling heat transfer of refrigerant R32 in the same internal micro-finned tube under varying heat flux densities.

2. Models and methods

2.1 Physical model

In order to simulate the flow boiling heat transfer process in the internal micro-finned tube, a corresponding three-dimensional geometric model was established. The model is an internal micro-finned tube with an inner diameter (tooth tip diameter) of 3.32mm and a length of 110mm. The rib shape is a trapezoidal rib with an apex angle of 40°. The specific parameters are shown in Table 1. The structure of the internal micro-finned tube is shown in Figure 1.

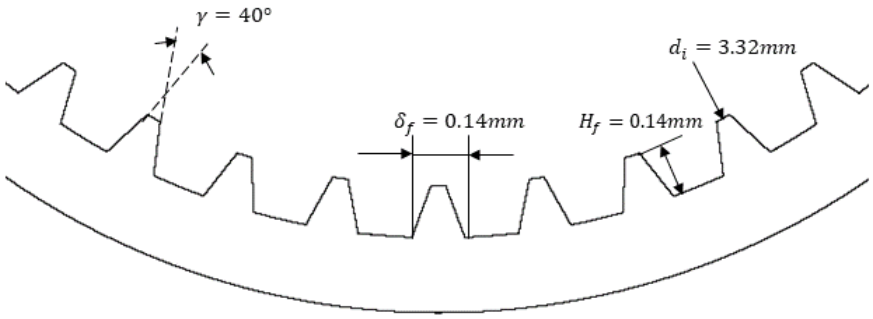

Figure 1. Schematic diagram of micro-fin tube structure.

Table 1. Model parameters.

Length(mm)	Tooth Tip diameter di(mm)	Number of teeth	Tooth height Hf(mm)	Tooth tip angle Γ(°)	Helix angle (°)
110	3.32	40	0.14	40	18

2.2 Governing equations

This article utilizes the multiphase flow Volume of Fluid (VOF) model to analyze flow boiling heat transfer. Due to the complexity of the process, turbulence calculations are employed to accurately predict the process. This study uses the SST k-ω turbulence model. The phase transition model used in this article is the Lee model.

2.3 Boundary conditions and algorithm settings

In this paper, the boundary conditions of Velocity-inlet, Pressure-outlet, and Wall were selected for the entrance, exit, and wall, respectively. Among these, the wall was a uniform heat flow boundary condition. The physical properties of the refrigerant in the calculation domain (R32, R410A and R1234ze Vapor and liquid) are determined by the physical property query software REFPOP 8.0. Firstly, the gas phase distribution, heat transfer coefficient, and local pressure drop of different refrigerants R32, R410A, and R1234ze are obtained when the heat flux is 10kW/m^2, the mass flow

rate is 200kg/(m^2 s), the saturation temperature is 288.15K, and the inlet temperature is 288.15K. Then, the heat transfer characteristics and pressure drop characteristics of R32 under different heat flux densities are obtained when the heat flux of R32 is 10kW/m^2, 50kW/m^2, and 100kW/m^2, with the mass flow rate, saturation temperature, and inlet temperature remaining constant at 200kg/(m^2 s), 288.15K, and 288.15K respectively.

The algorithm is configured as follows: The pressure is in discrete format using PRESTO! The pressure-velocity coupling is in Fractional Step format, the volume fraction equation utilizes the Geo-Reconstruct algorithm, the momentum equation, the two turbulence equations, and the energy equation are all in second-order upwind format. The time step is set at 1×10^{-6}s.

3. Results and discussion

3.1 Distribution of flow patterns in tubes

3.1.1 Flow pattern distribution of different refrigerants in the tube.

Figure 2 shows the flow pattern variation of X=0 section in a 3.32mm diameter internal micro-finned tube with a mass flow rate of 200 kg/(m^2·s) and heat flux of 10 kW/m^2 for three different refrigerants, R32, R410A and R1234ze, respectively.

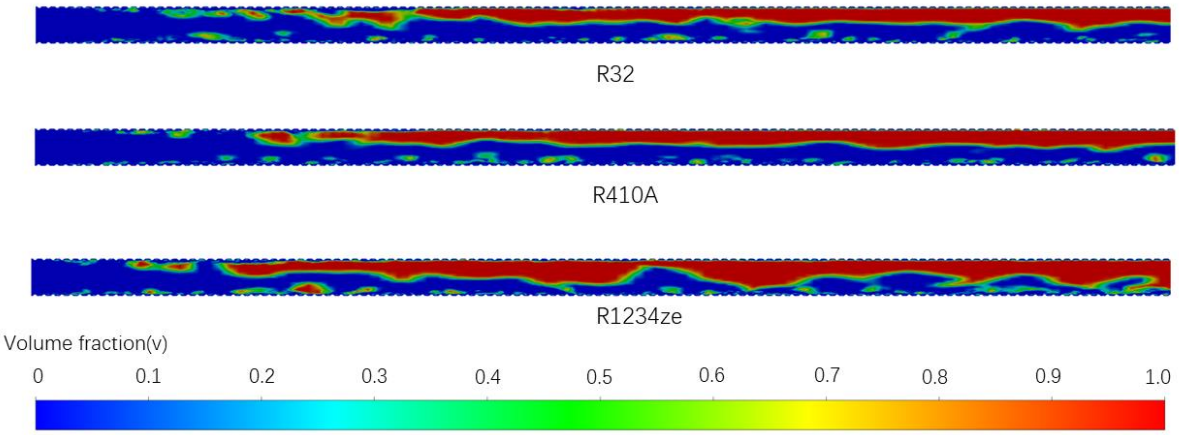

Figure 2. Distribution of gas phase volume fractions of different refrigerants in an internal micro-finned tube. (b) Distribution of the gas phase volume fraction at different cross-sections in an R32 internal micro-finned tube.

Observing Figure 2, we can see that bubble flow, slug flow, and wavy-annular flow appear in sequence when different refrigerants flow and boil in the pipe. Since the inlet temperature is the saturation temperature, the single-phase flow length is very short, and the refrigerant evaporates quickly. First, small bubbles appear.

As the evaporation proceeds, the bubbles continue to merge and become larger, gradually transitioning to a slug flow, and then a wavy-annular flow. Due to the influence of gravity, the density of the gas phase is lower than that of the liquid phase, and the gas phase is mainly distributed in the upper part of the internal micro-finned tube.

3.1.2 R32 flow pattern distribution at different cross-sections in the tube.

Figure 3 shows the distribution cloud diagram of the gas phase volume fraction of the cross-section of refrigerant R32 at different positions from the inlet of the internal micro-finned tube.

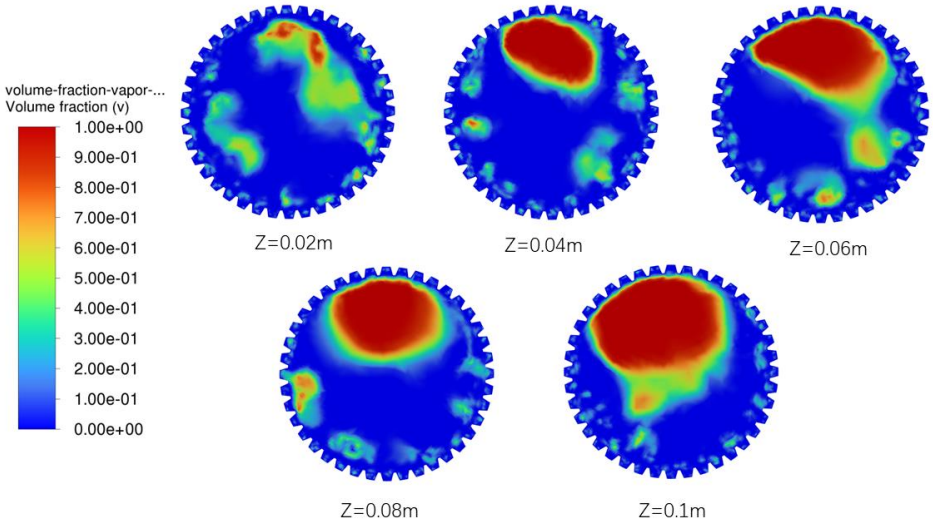

Figure 3. Distribution of the gas phase volume fraction at different cross-sections in an R32 internal micro-finned tube.

Observing Figure 3, we can see that as evaporation proceeds, the gas phase content in the internal micro-finned tube gradually increases, and the gas phase volume fraction continues to increase along the flow direction. The distribution of the two phases is asymmetric, with no obvious boundaries, and the gas phase is mainly concentrated in the middle area, with less content near the wall. Due to the influence of gravity, the density of the gas phase is lower than that of the liquid phase, and it is mainly distributed in the upper part of the tube.

3.2 Heat transfer characteristics of flow boiling in micro-finned tubes

3.2.1 Effect of refrigerant on heat transfer coefficient.

Figure 4 (a) shows the variation of boiling heat transfer coefficient of different refrigerants R32, R1234ze(E) and R410A under the conditions of saturation temperature of 288.15K, mass flow rate of 200 kg/(m^2·s) and heat flux of 10 kW/m^2, respectively. The horizontal axis represents dryness (x), while the vertical axis represents boiling heat transfer coefficient (h).

The analysis in Figure 4 (a) reveals that as dryness gradually increases, the boiling heat transfer coefficient of the working fluid R32 is the largest in the low dryness bubble flow area, while the boiling heat transfer coefficient of R1234ze is the smallest. It is evident that the boiling heat transfer coefficient varies among different refrigerants. The maximum boiling heat transfer coefficient of R32 is 25% higher than that of R410A, and the maximum boiling heat transfer coefficient of R410A is 3% higher than that of R1234ze.

This is because the physical properties of different refrigerants vary. The latent heat of evaporation of refrigerant R32 is higher, and its liquid thermal conductivity is also greater. When the liquid undergoes a phase change, the heat absorbed will be higher, resulting in a better heat transfer effect and a correspondingly higher boiling heat transfer coefficient. It is important to note that the latent heat of evaporation and liquid thermal conductivity of refrigerants R410A and R1234ze are lower than that of R32.When the liquid undergoes phase change, the heat absorbed will also be small, causing the boiling heat transfer coefficient to be less than R32. The heat transfer coefficient is proportional to the latent heat of evaporation and the liquid thermal conductivity.

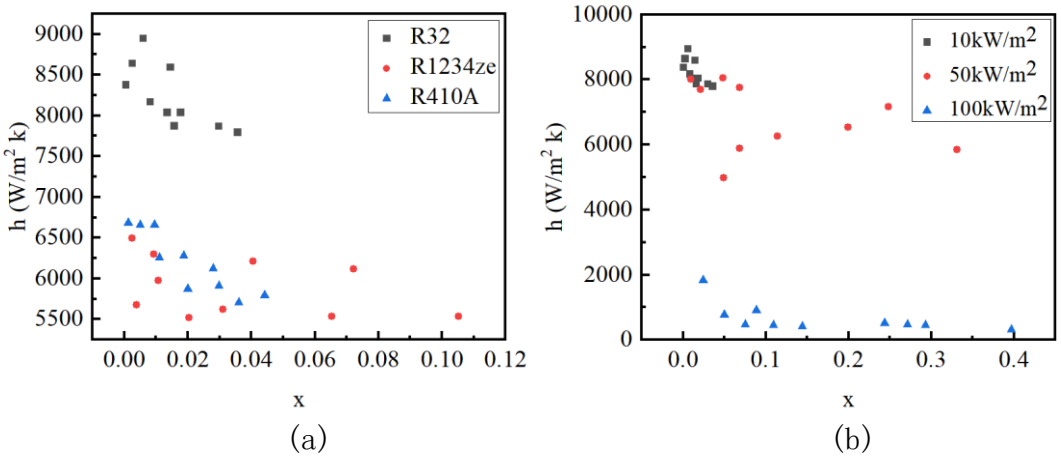

Figure 4. (a)The chart shows the variation of heat transfer coefficient with dryness under different refrigerants. (b)The Variation of heat transfer coefficient with dryness at different heat flux densities.

3.2.2 Influence of heat flux on heat transfer coefficient.

Figure 4 (b) shows the variation of heat transfer coefficient of refrigerant R32 with dryness under different heat flux densities. The horizontal axis represents dryness (x), while the vertical axis represents boiling heat transfer coefficient (h).

According to the analysis in Figure 4 (b), the heat transfer coefficient decreases with the increase of heat flux and gradually increases with the dryness. In the low dryness region, the boiling heat transfer coefficient has little change with dryness x. The boiling heat transfer coefficient of R32 with a heat flux density of 10 kW/m^2 is about 1 kW/ (m^2·K) and 7 kW/ (m^2·K) higher than that of 50 kW/m^2 and 100 kW/m^2. The boiling heat transfer coefficient of R32 at higher heat flux is much lower than that at lower heat flux.

This is because at higher heat flux levels, the temperature in the tube continues to rise, causing the droplet to almost completely evaporate, resulting in the phenomenon of "evaporation". The surface heat transfer coefficient decreases to its lowest point, leading to a deterioration in heat transfer. The gas content of the refrigerant in the pipe hardly changes, so the surface heat transfer coefficient gradually becomes stable.

3.3 Pressure drop characteristics of flow boiling in micro-finned tubes

3.3.1 Effect of refrigerant on pressure drop.

Figure 5 (a) shows the variation law of local pressure drop with pipe length for refrigerants R32, R410A and R1234ze under the condition of saturation temperature of 288.15K, mass flow rate of 200 kg/(m^2·s), and heat flux of 10 kW/m^2. In the figure, the horizontal coordinate is the distance from the inlet, represented by l, and the vertical coordinate is the pressure drop, represented by ΔP.

As can be seen from Figure 5 (a), R1234ze has the highest average pressure drop, followed by R32 and R410A. This is because the different thermophysical properties of different refrigerants lead to different pressure drops. At the saturation temperature of 288.15K, the liquid density and liquid viscosity of R1234ze are higher than those of R32. Additionally, the average pressure drop of R1234ze is 30% higher than that of R32. On the other hand, the liquid density and vapor density of R32 are both lower than those of R410A. Similarly, the liquid viscosity and vapor viscosity of R32 are also lower than those of R410A. However, the boiling heat transfer coefficient of R32 is larger, resulting in more intense boiling heat transfer. This leads to the average pressure drop of R32 being 8.8% higher than that of R410A. These differences in properties are the reasons for the varying pressure drops.

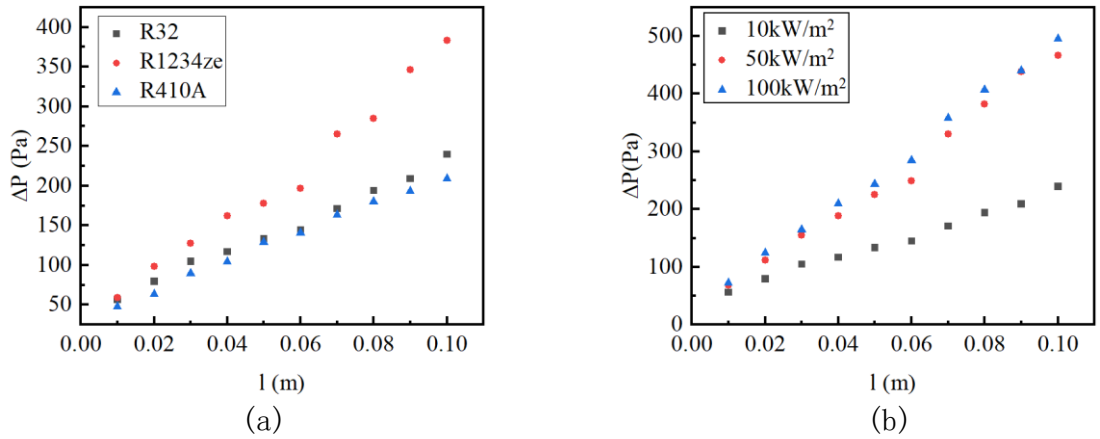

Figure 5. (a) A diagram illustrating the relationship between pressure drop and tube length for various refrigerants is shown. (b) A diagram illustrating the relationship between pressure drop and tube length at varying heat flux levels is presented.

3.3.2 Effect of heat flux on pressure drop.

Figure 5 (b) shows the variation of local pressure drop with pipeline length when the heat flux of refrigerant R32 is 10 kW/m^2, 50 kW/m^2 and 100 kW/m^2, respectively. In the figure, the horizontal coordinate is the distance from the inlet, represented by l, and the vertical coordinate is the pressure drop, represented by ΔP.

It can be seen from Figure 5 (b) that the pressure drop increases with the increase of heat flux. The largest pressure drop is 100kW/m^2, followed by 50kW/m^2 and 10kW/m^2.This is because when the heat flux is large, the heat transfer is also large, which results in an increase in the steam mass. With the same mass flow rate, the gaseous density decreases and the speed increases, leading to an overall increase in the fluid speed and ultimately causing an increase in the pressure drop in the flow process.

By observing Figures 5, it can be seen that the local pressure drop increases with the length of the pipeline. This is because as the refrigerant flows through the pipe, it generates friction resistance against the inner wall, leading to a gradual decrease in the pressure of the working fluid. Due to the presence of ribbed surfaces in internal micro-finned tubes, the pressure drop is more significant. In addition, when the temperature of the working fluid increases, it will evaporate to form a gaseous working fluid, and the gas content increases, thereby increasing the flow rate of the working fluid, ultimately leading to an increase in the pressure drop during the flow process.

4. Conclusion

The VOF model was utilized to perform a numerical simulation study on boiling heat transfer using various refrigerants and refrigerant R32 at different heat flux densities within an internal micro-finned tube with a 3.32mm inner diameter. The study yielded data on gas phase distribution, heat transfer coefficient, and local pressure drop for the different refrigerants and refrigerant R32, leading to the following conclusions:

a) As evaporation proceeds, the gas phase content in the internal micro-finned tube gradually increases, mainly concentrated in the middle area, with less content near the wall. Due to the influence of gravity, the gas phase is mainly distributed in the upper part of the tube; When different refrigerants flow and boil in the pipeline, bubble flow, slug flow, and wavy-annular flow appear successively.

b) The boiling heat transfer coefficient of the working fluid R32 is the largest, and the boiling heat transfer coefficient of R1234ze is the smallest. The boiling heat transfer coefficient is proportional to the latent heat of evaporation and the liquid thermal conductivity; The heat transfer coefficient decreases with the increase of heat flux density.

c) The local pressure drop increases as the pipe length increases; R1234ze has the largest average pressure drop, followed by R32 and R410A, which is related to the density, viscosity and heat transfer intensity of the refrigerant; The pressure drop increases with the increase of heat flux density.

References

[1] YU J, LI Z, CHEN E, et al. Experimental assessment of solar absorption-subcooled compression hybrid cooling system [J]. Solar Energy, 2019, 185: 245-54.

[2] XIE Y, ZHAO Y, LIU G, et al. Annealing Effects on XLPE Insulation of Retired High-Voltage Cable [J]. IEEE Access, 2019, 7: 104344-53.

[3] WANG P-Y, MA H, LIU G, et al. Dynamic Thermal Analysis of High-Voltage Power Cable Insulation for Cable Dynamic Thermal Rating [J]. IEEE Access, 2019, 7: 56095-106.

[4] JING Y, LI Z, LIU L, et al. Exergoeconomic-optimized design of a solar absorption-subcooled compression hybrid cooling system for use in low-rise buildings [J]. Energy Conversion and Management, 2018, 165: 465-76.

[5] RIGHETTI G, LONGO G A, ZILIO C, et al. R1233zd(E) flow boiling inside a 4.3 mm ID microfin tube [J]. International Journal of Refrigeration, 2018, 91: 69-79.

[6] KONDOU C, BABA D, MISHIMA F, et al. Flow boiling of non-azeotropic mixture R32/R1234ze(E) in horizontal microfin tubes [J]. International Journal of Refrigeration, 2013, 36(8): 2366-78.

[7] LONGO G A, MANCIN S, RIGHETTI G, et al. Comparative analysis of microfin vs smooth tubes in R32 and R410A boiling [J]. International Journal of Refrigeration, 2021, 131: 515-25.

[8] YANG C-Y, NALBANDIAN H, LIN F-C. Flow boiling heat transfer and pressure drop of refrigerants HFO-1234yf and HFC-134a in small circular tube [J]. International Journal of Heat and Mass Transfer, 2018, 121: 726-35.

[9] JIGE D, SAGAWA K, IIZUKA S, et al. Boiling heat transfer and flow characteristic of R32 inside a horizontal small-diameter microfin tube [J]. International Journal of Refrigeration, 2018, 95: 73-82.

[10] MING-HUEI YU* T-K L, CHYUAN-CHYI TSENG. Heat transfer and flow pattern during two-phase flow boiling of R-134a in horizontal smooth and microfin tubes [J]. 2002.

[11] KATTAN N, THOME J R, FAVRAT@IT.DGM.EPFL.CH, et al. Flow Boiling in Horizontal Tubes: Part 3—Development of a New Heat Transfer Model Based on Flow Pattern [J]. 1998.